

Influence of Iron Powder Properties on Hysteresis Loss of Iron Powder Core[†]

TAKASHITA Takuya^{*1} NAKAMURA Naomichi^{*2} OZAKI Yukiko^{*3}

Abstract:

The crystal grains in an iron powder core, made from an insulation coated iron powder through a compaction process, recrystallize into smaller grains during stress relief annealing after the compaction. In this study, the method to suppress the recrystallization is investigated to reduce the hysteresis loss of the iron powder core. The iron powder properties have an influence on the recrystallization behavior: an iron powder core with coarser crystal grain size is obtained by a decrease in the compaction strain acting as the recrystallization nucleus due to an increase in apparent density, average particle diameter, and crystal grain size of the iron powder. In addition, recrystallized grain growth is accelerated by reduction of impurity in the iron powder. The iron loss of the iron powder core with crystal grain size of 37 μm shows an iron loss lower than that of a typical electrical steel core with a thickness of 0.35 mm.

1. Introduction

According to the requirement for reduction of environmental loads and energy conservation, there has been an orientation toward downsizing and higher efficiency in electromagnetic parts in recent years. In comparison with conventional stacked electrical steel sheets, iron powder cores have the advantage of a high degree of freedom for shape design. Utilizing this advantage, development related to downsizing of motors which use 3-dimensional magnetic circuits has progressed in some respects¹⁾. Although Fe-Si powder, Fe-Si-Al powder, Fe-Ni powder, pure iron powder, etc. are known as magnetic powders that can be used as raw materials for iron

powder cores, among these, pure iron powder has the merit that a high magnetic flux density is easily obtained as high densification of the iron powder cores is possible.

Iron loss is one of the properties which is required in soft magnetic materials. Iron loss is the loss that occurs when a soft magnetic material converts electrical energy to magnetic energy. Iron loss can be further divided into hysteresis loss and eddy current loss. Because the particles in an iron powder core are coated individually with an insulating coating, eddy current loss of iron powder cores is low in comparison with that of stacked steel sheets. On the other hand, it is necessary to reduce the hysteresis loss of iron powder cores, which is high in comparison with that of steel sheets.

Hysteresis loss increases with an increase in strain, crystal grain boundaries and inclusions in the microstructure²⁾. Since pure iron powder cores are manufactured by compaction of the iron powder followed by stress relief annealing, the powder properties of their iron powder are considered to have a large influence on the properties of the iron powder core. Therefore, in this research, the influence of the apparent density, average particle size, crystal grain size and purity of the iron powder on the hysteresis loss of iron powder cores was investigated. As a result, it was found that all of these factors cause changes in hysteresis loss by way of actions that cause changes in the crystal grain size of iron powder cores after annealing. The details of that study are reported in the following.

[†] Originally published in *JFE GIHO* No. 36 (Aug. 2015), p. 75–81



^{*1} Senior Researcher Assistant Manager,
Iron Powder & Magnetic Materials Res. Dept.,
Steel Res. Lab.,
JFE Steel



^{*2} Dr. Eng.,
Senior Researcher Deputy General Manager,
Iron Powder & Magnetic Materials Res. Dept.,
Steel Res. Lab.,
JFE Steel



^{*3} Dr. Sci.,
General Manager, Iron Powder & Magnetic Materials
Res. Dept.,
Steel Res. Lab.,
JFE Steel

2. Experimental Method

2.1 Iron Powders

The powder properties of the iron powders used in this research are shown in **Table 1**. All of the iron powders were produced by the water atomizing process. Apparent density was varied by adjusting the atomizing conditions. After atomizing, the powders were annealed in a H_2 atmosphere, followed by adjustment of the particle size by sieving. In the case of iron powders D3' and E, second annealing was performed in H_2 under conditions of a soaking temperature of 1 323 K and soaking time of 5.4 ks for increasing the crystal grain size.

The average particle size (D_{50}) of the iron powders A, B, and C obtained by the sieving was the same, but their apparent densities were different, the highest being A, 4.07 Mg/m^3 and the lowest being C, 3.19 Mg/m^3 . Focusing on the cross-sectional photographs shown in **Photo 1**, it can be understood that the particle cross sec-

tions of A, B, and C approach a circular shape as the apparent density of the powders increases. The crystal grain size measured from the cross-sectional photos by the intercept method³⁾ is approximately $40 \mu\text{m}$ for all of the iron powders A, B, and C. The results of same measurements of the crystal grain sizes of the other iron powders are also shown in Table 1. In D1 to D3, the crystal grain size increases as D_{50} increases, and the crystal grain size of D4 is approximately the same as that of D3. Although the particle sizes of D3' is the same as that of D3, the crystal grain size of D3' is $66.7 \mu\text{m}$, which is $16.2 \mu\text{m}$ larger than that of D3.

The amount of impurity of iron powder E is 1/10 that of the other iron powders. Here, "amount of impurity" indicates the total amount of Si, Al, Mn, and Cr, which are considered to increase hysteresis loss by oxidizing and forming inclusion during water atomizing. The crystal grain size of E is $66.5 \mu\text{m}$, which is approximately the same as that of D3'.

2.2 Powder Core Fabrication Method

The respective iron powders were mixed with silicon resin (SR 2400, manufactured by Dow Corning Toray Co., Ltd.) so as to obtain a resin ratio of 0.25 mass% by solid content, and coating treatment was then performed by drying for 43.2 ks in air at room temperature. Following this, the coated powders were heat-treated at 473 K in air for 7.2 ks to harden the coated resin. The coated iron powder after hardening treatment was compacted in a ring shape (Outer diameter: 38 mm, Inner diameter: 25 mm, Height: 6 mm) by the die wall lubrication compaction method. The compacting pressure was adjusted to obtain a density of 7.45 Mg/m^3 . A suspension consisting of zinc stearate dispersed in ethanol was used as the lubricant. The lubricant was coated with a brush on the die surface. The powder cores prepared by this method (hereinafter, "as-compacted iron powder

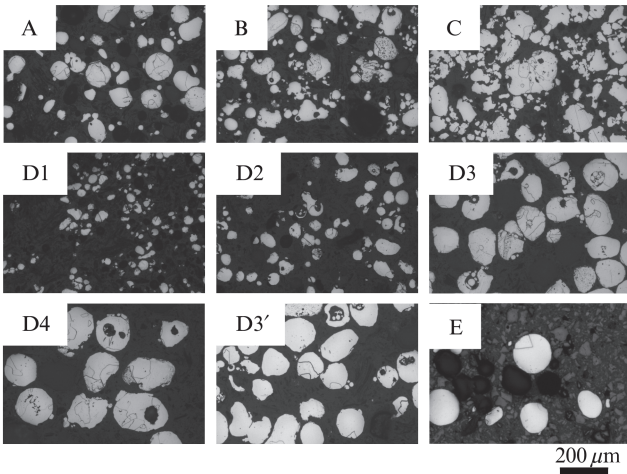


Photo 1 Optical micrograph of iron powders (Nital etching)

Table 1 Powder properties of iron powders

Based iron powder	Re-annealing for powder	Apparent density, AD (Mg/m^3)	Particle size distribution (mass%)					Amount of impurity (Si, Mn, Al, Cr) (mass%)	Average particle size, D_{50} (μm)	Crystal grain size, d (μm)
			250–180 μm	180–150 μm	150–106 μm	106–45 μm	< 45 μm			
A	×	4.07	0.0	0.6	25.0	59.0	15.4	0.071	82.2	39.7
B	×	3.57	0.0	0.1	23.5	58.4	18.0	0.065	81.0	40.5
C	×	3.19	0.0	1.2	29.3	54.3	15.2	0.078	82.4	40.7
D1	×	3.72	0.0	0.0	0.0	0.0	100.0	0.088	22.5	18.9
D2	×	3.83	0.0	0.0	0.0	100.0	0.0	0.076	75.5	34.3
D3	×	3.93	0.0	0.0	100.0	0.0	0.0	0.076	128.0	50.5
D4	×	3.96	0.0	100.0	0.0	0.0	0.0	0.076	165.0	48.1
D3'	○	3.93	0.0	0.0	100.0	0.0	0.0	0.069	128.0	66.7
E	○	4.14	17.4	11.6	20.5	50.6	0.0	0.005	114.0	66.5

×: Not be carried out ○: Be carried out

core”) were subjected to stress relief annealing at a soaking temperature of 973 K for a soaking time of 2.7 ks in N_2 , and were then used as cores for evaluation (hereinafter, “core”).

2.3 Powder Core Evaluation Method

The density of the as-compacted cores was calculated from their dimensions and weights. The hysteresis loss of the cores was measured with a direct current magnetic property measuring equipment (type SK-110, manufactured by Metron, Inc.). Measurements were performed at the magnetic flux density of $B_m = 1.0$ T. Hysteresis loss per cycle was calculated from the obtained loop area, and the hysteresis loss at frequency $f = 1$ kHz was calculated by multiplying the result by 1 000. After the magnetic measurements, microstructural observation of the cores was performed with an optical microscope on the cross-section of the cores. **Table 2** shows the results of density measurements of the as-compacted cores. And the results of measurements of the hysteresis loss and results of intercept-method measurements of the crystal grain size of the cores. It can be understood that the density of the as-compacted cores is within a range of ± 0.1 Mg/m³. Furthermore, the hysteresis loss of the cores ranges from the minimum value of 41.6 W/kg for core 9 to the maximum value of 94.0 W/kg for core 4, and thus varied by more than 2 times depending on the iron powder. The crystal grain size also ranged from the minimum value of 13.0 μm in core 4 to the maximum value of 36.7 μm in core 9.

Micro Vickers hardness measurements were carried out for the particles in iron powders A, B, and C and the as-compacted cores obtained with those iron powders. In all cases, the measurements were performed at 5 positions in each sample in such a way that the indentation did not extend across the grain boundary, at the indentation load of 0.245 N. The minimum and maximum values were excluded, and the average of the remaining

3 measured values was obtained. The hardness difference between the as-compacted cores and the iron powder was defined as ΔH_V , and was used as an index of the density of the dislocations accumulated in the iron powder during compaction.

3. Results and Discussion

3.1 Influence of Apparent Density of Iron Powder on Microstructure of Iron Powder Cores

Photo 2 shows the results of microstructural observation of cores 1–3, which consist of iron powders A–C, which had the same value of D_{50} and different apparent densities. **Figure 1** shows the average crystal grain sizes measured by the intercept method using the cross-sectional photographs, together with the crystal grain sizes of the iron powders. It can be understood that the crystal grain size is smaller than that of the iron powder in all of the cores, but the crystal grain size of the cores increases with an increase in apparent density of the powder. **Figure 2** shows the relationship between apparent density and ΔH_V , which is the index of the density of dislocations accumulated during compaction, and **Fig. 3** shows the relationship between ΔH_V and the crystal grain size of the cores. From these figures, it can be understood that ΔH_V is decreased with an increase in the apparent density of the iron powder, and the crystal grain size after annealing increases with a decrease in

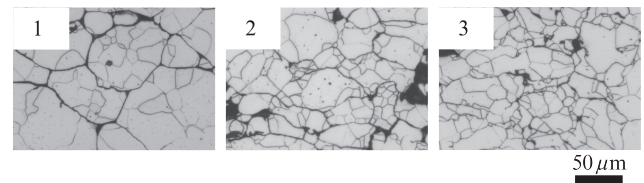


Photo 2 Optical micrographs of cores 1, 2, and 3 (Nital etching)

Table 2 Density and hysteresis loss of cores

Core	Used powder	Density (Mg/m ³)	Hysteresis loss, W_h (W/kg)	Crystal grain size, D (μm)
1	A	7.40	70.7	20.8
2	B	7.38	81.5	17.1
3	C	7.44	87.0	14.1
4	D1	7.46	94.0	13.0
5	D2	7.45	72.8	18.1
6	D3	7.40	65.4	21.4
7	D4	7.49	53.4	21.1
8	D3'	7.39	66.9	27.7
9	E	7.55	41.6	36.7

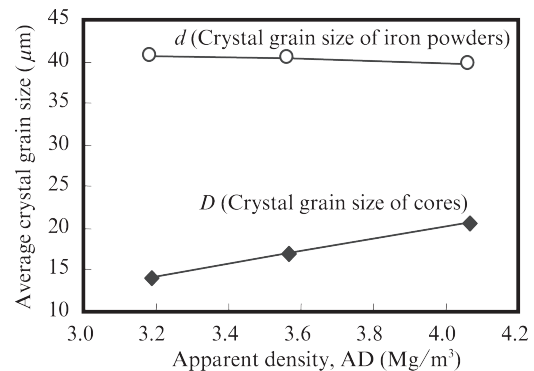


Fig. 1 Relationships between apparent density of iron powders and crystal grain size of iron powders and cores

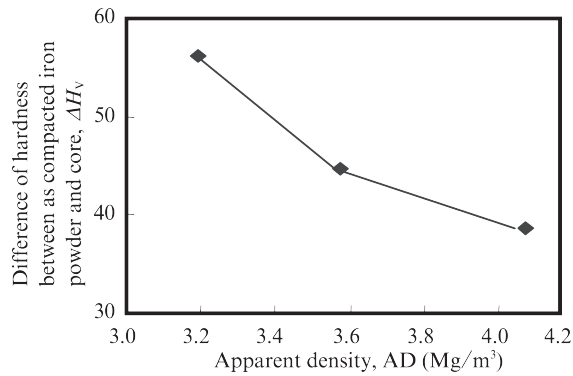


Fig. 2 Relationship between apparent density of iron powders and ΔH_v (Difference between iron powder and core as compacted)

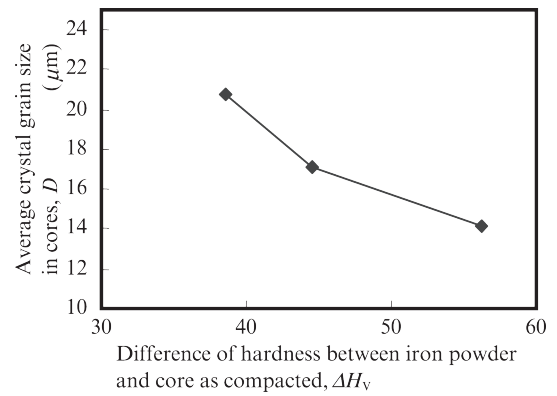


Fig. 4 Relationship between apparent density and an increase in density during compaction

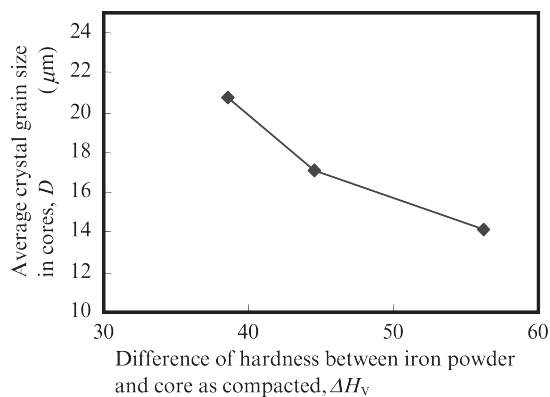


Fig. 3 Relationship between ΔH_v (Difference between iron powder and core as compacted) and crystal grain size in cores

ΔH_v .

The above-mentioned results show that accumulation of dislocations in the iron powder during compaction is decreased with an increase in the apparent density of the powder, and this results in refinement of the crystal grain size in the core after annealing. This behavior can be explained by recrystallization. That is, it is considered that dislocations accumulate during compaction, and formation of recrystallization nuclei occurs as a result of stress relief annealing. Furthermore, if the number of accumulated dislocations decreases, the amount of recrystallization nuclei formed during annealing will decrease and the crystal grain size will increase⁴⁾.

Next, the mechanism responsible for the decrease in the number of dislocations accumulated during compaction with an increase in apparent density will be considered. **Figure 4** shows the relationship between the apparent densities of iron powders A, B, and C and the difference in the densities of cores 1–3, in other words, the increase in density due to compaction. It can be understood that the increase in density accompanying compaction decreases in iron powders with higher

apparent densities. From this, assuming compaction to the same green density, it can be understood that an iron powder with a high apparent density can achieve the target density with a smaller amount of plastic deformation. From this, the increase in the crystal grain size accompanying the increase in the apparent density of the iron powder can be explained by the decrease in the dislocations accumulated during compaction, and suppression of the formation of recrystallization nuclei during stress relief annealing due to the reduction in dislocations.

3.2 Influence of Crystal Grain Size on Microstructure of Cores

Photo 3 shows the results of microstructural observation of cores 4–9, which consist of iron powders D1–D4 with different grain sizes, iron powder D3', which was produced by second annealing of D3, and iron powder E, which has a reduced content of impurities in comparison with the other iron powders. Among these, the results for core 9 will be discussed in the following Section 3.3. **Figure 5** shows the relationship between D_{50} and the average crystal grain size measured from the cross-sectional photographs of cores 4–8. In cores 4–7, the crystal grain size tends to increased due to the

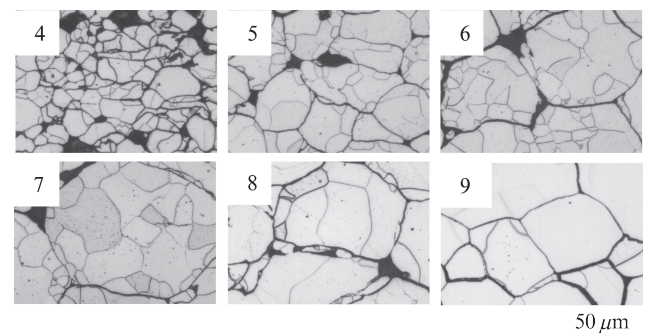


Photo 3 Optical micrographs of cores 4~9

increase in D_{50} in the iron powders. The following will discuss the cause of the change in the crystal grain size of the cores due to the change in D_{50} . Figure 6 shows the relationship between the crystal grain size of the iron powder and the crystal grain size in the core for cores 4–8. It can be understood that the crystal grain size of the cores increases as the average crystal grain size of the iron powder increases. Dislocations easily accumulate at grain boundaries during processing, and this region tends to become a site for the formation of recrystallization nuclei⁴⁾. Based on this fact, it is considered that that accumulation of dislocations in iron powder during compaction becomes more difficult as the crystal grain size of the iron powder becomes coarser, and as a result, refinement of crystal grains by recrystallization is suppressed.

Core 8 has the same D_{50} and apparent density as core 6, but the crystal grain size of the iron powder is different. When the arranged by D_{50} , as in Fig. 5, the plot for this core deviates from the line formed by cores 4–7. However, when arranged by the crystal grain size of the iron powder, as in Fig. 6, all of the plots of cores 4–8 lie on a straight line. From this, it can be understood that the crystal grain size of the iron powder influences the

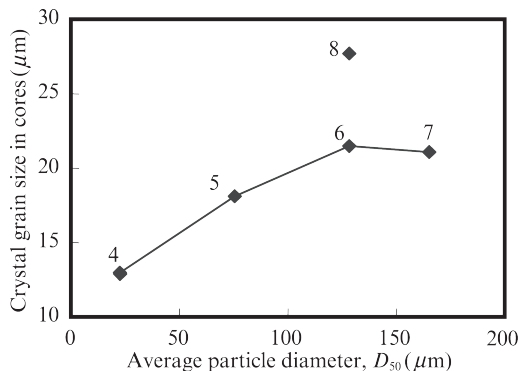


Fig. 5 Relationship between D_{50} of iron powders and crystal grain size in cores

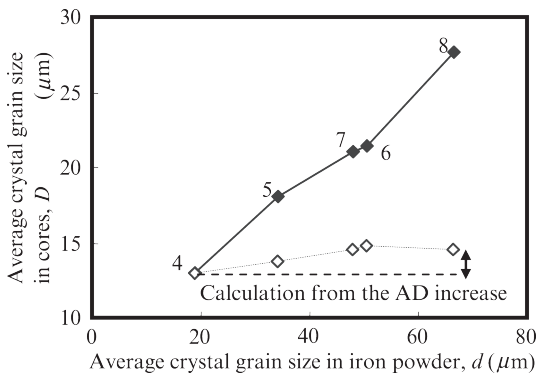


Fig. 6 Relationship between crystal grain size in iron powders and crystal grain size in cores

crystal grain size of the cores in the case of cores 4–8.

On the other hand, the apparent density of cores 4–8 also changes simultaneously with the D_{50} of the iron powder. Therefore, in the following, the authors attempted to separate the contributions of D_{50} and apparent density to the crystal grain size in the cores. In the series in which D_{50} is the same, which is shown in Fig. 1, the average crystal grain size of the cores changes linearly with changes in the apparent density AD of the iron powder. Therefore, when the slope of the change in AD was calculated by regression, it was estimated that the crystal grain size increases by $7.6 \mu\text{m}$ for each 1 Mg/m^3 increase in apparent density.

$$\Delta D = 7.6 \cdot \Delta AD \dots\dots\dots (1)$$

Where, ΔD is the increase in the crystal grain size of the core due to the increase of apparent density, and ΔAD is the increase of the apparent density of the iron powder. The following discussion is based on the assumption that the relationship in Eq. (1) is materialized independent of D_{50} . The broken line in Fig. 6 shows the results of the change in crystal grain size due to increased apparent density estimated by Eq. (1), normalized to core 4, which had the smallest apparent density of the iron powders among cores 4–8. This difference between the measured value and the contribution of the increase of apparent density calculated by Eq. (1) is considered to represent the contribution of D_{50} .

Accordingly, even if the contribution of apparent density is excluded, D_{50} causes the crystal grain size of the cores to increase by way of an increase in the crystal grain size of the iron powder. Thus, it is thought that the crystal grain size of the cores increases as a result of the increase in the crystal grain size of the iron powder.

3.3 Influence of Purity on Microstructure of Iron Powder Cores

Photo 3 showed the results of microstructural observation of core 8, which consists of iron powder D3', together with the results for core 9, which was produced from iron powder E, in which the content of impurities was reduced in comparison with the other iron powders. The crystal grain size of the iron powders was the same in both of these cores because reannealed iron powders were used in both cores. The difference of apparent density ΔAD , of these iron powders was 0.21 Mg/m^3 , and the change of the crystal grain size ΔD obtained from Eq. (1) was estimated as $1.60 \mu\text{m}$. However, the crystal grain size of the core 9 measured from the photograph was $36.7 \mu\text{m}$, which is $9.0 \mu\text{m}$ larger than that of core 8. Accordingly, the difference of the crystal grain size of cores 8 and 9 cannot be explained by the difference in the apparent density or the difference in the crystal grain

size in the iron powder, which was examined up to Section 3.2, suggesting the influence of some other factor.

As argued up to Section 3.2, the crystal grain size of cores has a large influence on the recrystallization behavior which occurs during annealing after compaction. Because movement of grain boundaries occurs during the growth of recrystallization nuclei, growth is suppressed by precipitates, inclusions and solid solution elements, which impede grain boundary movement⁴⁾. Comparing the iron powders D3' and E, in iron powder E, the total contents of Si, Al, Mn, and Cr, which have higher affinity for oxygen than that of Fe, is reduced to 1/10 of the level in D3'. Based on this, it is estimated that the amount of inclusions formed during water atomization of iron powder E, which was used in the core 9, was small in comparison with that in the iron powder D3' of core 8, and the crystal grain size of core 9 increases because there are fewer impediments to the growth of recrystallization nuclei during annealing.

3.4 Influence of Microstructure on Hysteresis Loss of Iron Powder Cores

According to Takajo et al.⁵⁾, the hysteresis loss W_h of iron powder cores can be expressed by the following equation.

$$W_h = \frac{4c \cdot B \cdot H_c}{\rho} \dots\dots\dots (2)$$

Where, c is a constant which is determined by the shape of the hysteresis loop, B is magnetic flux density, H_c is coercivity and ρ is the density of the green compact. According to Pfeifer et al.⁶⁾, coercivity H_c is expressed by Eq. (3).

$$H_c = H_{ck} + H_{c_ex} \dots\dots\dots (3)$$

Where, H_{ck} is coercivity originating from pinning of magnetic domain walls by crystal grain boundaries, and H_{c_ex} is coercivity originating from domain wall pinning within grains by inclusions, strain or other factors. Mager et al.⁷⁾ proposed that the coercivity originating from domain wall pinning by crystal grain boundaries is proportional to the reciprocal of the crystal grain size and can be expressed by the following equation.

$$H_{ck} \approx \frac{3 \cdot \gamma}{J_s \cdot D} \dots\dots\dots (4)$$

Where, γ is domain wall energy, J_s is saturation magnetization and D is the crystal grain size. When Eqs. (3) and (4) are substituted into Eq. (2), the following equation is obtained.

$$W_h = \frac{4c \cdot B}{\rho} \left(\frac{3 \cdot \gamma}{J_s \cdot D} + H_{c_ex} \right) \dots\dots\dots (5)$$

B is determined by the measurement conditions, and γ and J_s are characteristic values of the material. Assuming that H_{c_ex} , c and ρ are constants, it can be understood that hysteresis loss displays a linear relationship with the reciprocal of the crystal grain size. From the study up to this point, it has been suggested that the powder properties, microstructure and purity of the raw material iron powder influence the crystal grain size of cores. Therefore, in the following, the relationship between hysteresis loss and the crystal grain size of cores will be examined.

Figure 7 shows the relationship between the inverse the crystal grain size in cores and hysteresis loss. When a linear regression equation was prepared using these plots, a high correlation was obtained, as the correlation coefficient $R^2 = 0.97$. This demonstrates quantitatively that the properties and microstructure of the green compact of the iron powder influence the crystal grain size when iron powder is used in a core, and hysteresis loss is reduced through an increase in crystal grain size. In order to investigate the influence of impurities, a multiple regression analysis was carried out using the reciprocal of the crystal grain size and the content of impurities of all of the cores, but it was not possible to obtain significant results which mean that the content of impurities influences hysteresis loss. Therefore, within the range of this study, it is thought that the contribution of intragranular pinning by inclusion, etc. was constant in all of the specimens. This is presumably because the sizes of the intragranular pinning sites (inclusions, etc.) due to impurities in the iron powders used in these experiments were smaller than the minimum size ($0.5 \mu\text{m}$)⁸⁾ at which pinning of domain walls is possible. Accordingly, the authors conclude that, within the range of the present study, hysteresis loss was attributable mainly to changes in the crystal grain size in the cores.

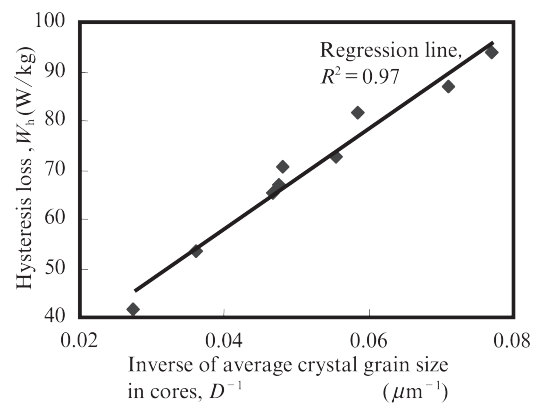


Fig. 7 Relationship between inverse of crystal grain size in cores and hysteresis loss

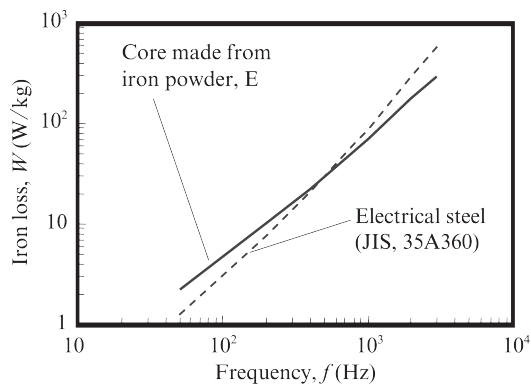


Fig. 8 Iron loss of the core 9 and electrical steel

3.5 Comparison of Iron Loss of Iron Powder Cores and Electrical Steel Sheets

Finally, Fig. 8 shows the results of a comparison of the iron loss of core 9, which displayed the lowest hysteresis loss in this study, and an electrical steel sheet (JIS Standard 35A360, JIS: Japanese Industrial Standards). Measurements were performed after forming the sheet into a ring shape with an outer diameter of 38 mm and an inner diameter of 25 mm by electrical discharge machining and then winding the specimen. The excitation magnetic flux density was 1.0 T, and measurements were performed from the frequency of 50 Hz to 3 kHz. The iron loss of the electrical steel sheet was lower than that of the core 9 up to the frequency of 800 Hz, but above 800 Hz, the iron loss of the core 9 was lower. Based on this result, in high speed motors, etc. with core excitation frequencies exceeding 800 Hz, improved motor efficiency is expected by using iron powder cores made from iron powder E in comparison with motors made from electrical steel sheets.

4. Conclusion

In this study, the influence of the powder properties of iron powders on the microstructure and hysteresis loss of cores was studied, and the following knowledge was obtained.

- (1) Apparent density: Plastic deformation of the powder during compaction is suppressed and accumulation of dislocations during compaction is reduced by

increasing the apparent density of the iron powder. This in turn suppresses the formation of recrystallization nuclei during annealing, and thereby increases the crystal grain size in the core.

- (2) Powder particle size and crystal grain size of powder: An increase in the size of powder particles and annealing the powder increases the crystal grain size of the powder. An increase in the powder crystal grain size reduces the number of grain boundaries, where dislocations easily accumulate, and thereby reduces the number of dislocations which accumulate during compaction. This suppresses the formation of recrystallization nuclei during annealing and increases the crystal grain size in the core.
- (3) Purity: Reducing the content of impurities in the powder promotes the growth of recrystallization nuclei during annealing and increases the crystal grain size of the core. The hysteresis loss of the cores prepared in the study of the above (1) through (3) was reduced by the increase in crystal grain size. This shows a universal behavior which can be explained by a grain boundary pinning model.
- (4) Iron loss of iron powder cores and stacked electrical steel sheets: Among the cores 9 which were trial-manufactured in this study, the core with the coarsest crystal grain size, namely, $36.7 \mu\text{m}$, displayed lower iron loss than a general electrical steel sheet at frequencies exceeding 800 Hz.

Based on the knowledge obtained in this research, further reductions in the iron loss of iron powder cores is expected by optimizing the powder properties of the iron powder (increasing the apparent density and crystal grain size of the powder, reducing the impurity content).

References

- 1) Hultman, Lars et al. Advances in powder metallurgy & particulate materials. 2002, p. 14–26.
- 2) Ohta, K. Jikikougakunokiso II. Kyoritsu Shuppan, 1973, p. 296.
- 3) Fullman, R. L. Trans. AIME. 1953, p. 197–447.
- 4) Furubayashi, E. Saikessyoutozairyouosshiki. Uchida Rokakuho, 2000, p. 29–31.
- 5) Takajo, S. Tohoku Univ., 1986. Doctorial Theses.
- 6) Pfeifer, F.; Radeloff, C. Journal of Magnetism and Magnetic Materials. 1980, vol. 19, p. 190–207.
- 7) Mager, A. Annalen der Physik. 1952, vol. 6, p. 15–16.
- 8) Hara, T.; Shigetomi, T.; Okiyama, T.; Takemoto, T. J. Japan Inst. Metals. 1997, vol. 61, p. 553–560.